Ain Shams Engineering Journal 11 (2020) 1035–1046

Contents lists available at ScienceDirect

Ain Shams Engineering Journal

journal homepage: www.sciencedirect.com

Civil Engineering

Hydrodynamic modeling for identifying flood vulnerability zones in lower Damodar river of eastern India

Ravindra Kumar Singh [a], Vasanta Govind Kumar Villuri [b], Srinivas Pasupuleti [c,*], Rajesh Nune [d]

[a] Department of Civil Engineering, Indian Institute of Technology(ISM), Dhanbad 826004, India
[b] Department of Mining Engineering, Indian Institute of Technology(ISM), Dhanbad 826004, India
[c] Department of Civil Engineering, Indian Institute of Technology(ISM), Dhanbad 826004, India
[d] ICRISAT Development Center, International Crops Research Institute For The Semi Arid Tropics, Patancheru, Hyderabad 502324, India

A R T I C L E I N F O

Article history:
Received 29 September 2019
Revised 2 December 2019
Accepted 13 January 2020
Available online 6 March 2020

Keywords:
Flood
Hydrodynamic model
MIKE HYDRO RIVER
Damodar river
DHI

A B S T R A C T

The identification of flood vulnerability zone is very essential to minimize the damage associated with the flood. The present study adopted the Hydrodynamic modeling technique for the identification of flood vulnerability zones in lower Damodar river of eastern India. Preprocessing of data and preparation of various input geometry data (river network, bank line) for the hydrodynamic model were done in an ArcGIS environment with the help of high resolution satellite imagery and field survey. Model was calibrated for the Manning's coefficient of roughness (n) and validated with ground data and field photographs high-resolution, the efficiency of the model was estimated by the index of agreement "d" which clearly shows good agreement between model data and observed data. Based on the model output flooding hotspots were demarcated. It was observed that areas downstream to the bifurcation point of the Damodar river are more vulnerable to flooding.

1. Introduction

Floods are an unavoidable natural hazard, which not only causes human loss but also loss of natural resources, thereby loss of wealth to the nation [1]. A large portion of India exclusively eastern portion is under the risk of flooding during southwest monsoon [1–3]. The flood may be coastal, surface and riverine which depends on hydrological and topographical conditions. The cyclonic storm caused huge damage in the coastal region and low laying areas inundated due to these storms. Some researchers used computational fluid dynamics (CFD) techniques to study fluid flow and other associated parameters in the cyclone domain [4]. Natural and anthropogenic activities near a river system, drainage congestion in low laying areas, siltation in the river and improper flood management approach are some basic causes that create flooding situations [5]. In the hilly region during major flood times, the scouring of river bed takes place, which ultimately changes the step-pool morphology of steep mountain streams. [6] shows the strong correlation between several morphological parameters of the river of the step-pool morphology in their study.

Flood risk management comprises the procedure of hazard evaluation, executing and exploring alternatives to diminish the damages of flooding [7,8]. Understanding of 1-D, as well as the 2-D Spatio-temporal variation of flood flow aids in the decision-making process to combat flood disasters [5,8]. Also, knowledge of high-velocity jet impact on scouring and effects of bed topography at downstream of dams [9] and understanding of the effect of entrance flow conditions on the pressure fluctuation is very important for the protection of large dams [10], which helps in some extent to minimize the magnitude of flood. Numerous scholars for hydrological studies adopted either deterministic or stochastic approaches to achieve their objective. [11] developed stochastic models for prediction of a flood using Box-Jenkins methodology in the Karkheh river basin in Khuzestan state in Iran. Hydrodynamic models perform a key role in suggesting preventive measures for flood management by identifying flooding risk hotspots [12–14]. A hydrodynamic modeling approach was widely used by

* Corresponding author.
E-mail addresses: ravindrain11.2016dr48@cve.ism.ac.in (R.K. Singh), vgkvilluri@iitism.ac.in, vgkvilluri@iitism.ac.in (V.G. Kumar Villuri), srinivas@iitism.ac.in (S. Pasupuleti), R.Nune@cgiar.org (R. Nune).

Peer review under responsibility of Ain Shams University.

Production and hosting by Elsevier

https://doi.org/10.1016/j.asej.2020.01.011
2090-4479/

various researchers to study flood inundation in the floodplains [15–17]. Remote sensing data and GIS applications help in knowing the extent of flooding, flood damage assessment, floodplain mapping, etc. [18,19]. Some investigators used Synthetic Aperture Radar (SAR) imagery to study floodplain inundation dynamics [20]. The modeling procedure of flood inundation principally comprises the solution of Saint-Venant equations using numerical techniques [21]. Evolution in modeling methods, ease of access of remote sensing data and progress of computer-executable systems reduced the flood inundation and river hydraulics study complexity to a certain extent [22–25]. However, resource availability is the main concern in this type of study since it is vastly influenced by topographic data, geometric arrangement, and modeling methods [15,26,27]. Poor maintenance and lack of good quality of observed data related to river hydraulics is the major constraint for the hydrodynamic modeling studies of riverine flooding in developing countries like India [5,26]. Lack of a sufficient number of river gauge stations and measured cross-sections in low laying floodplain areas restricted the flood modeling studies in these regions.

There are several techniques successfully applied for flood-related study that to be for global level, but Hydrodynamic modeling technique for identifying flood vulnerability zones in local scale using high-resolution digital elevation model (DEM), especially in flat regions of lower Damodar is still not adopted and is not found in literature as per the knowledge of authors. Keeping in view of the above concerns, the present work deals with the riverine flooding problem of the Damodar river with hydrodynamic modeling perspective. This study utilized the high-resolution CARTOSAT DEM for geometric data in the lack of a sufficient number of measured river cross-sections data in lower Damodar river. The 1-D hydrodynamic modeling was performed in MIKE HYDRO RIVER developed by the Danish Hydraulic Institute (DHI). Outcomes of this study can immensely aid the engineers and planners in policy decisions for combating the floods in the lower Damodar basin.

2. Study area and data used

The Damodar river basin geographically lies between 22°15′ to 24°30′N latitude and 84°30′ to 88°15′E longitude. The upper catchment of the Damodar river basin consists of hills, plateaus and sloping land, which are rich in mineral resources spreads in the state of Jharkhand, India. The lower catchment of the basin is a fertile stretch of agriculturally productive plain land in the state of West Bengal, India. The origin of the Damodar river is in the Palamu hills of Jharkhand. It joins with Barakar river just downstream to Panchet and Maithon dams. Damodar river bifurcates into two main streams, right stream Mundeswari and the left stream Amta Damodar below Paikpara [28–30]. During 1950, some large and medium-sized dams were built on the upstream catchment of the Damodar river basin to regulate floods mainly and for other purposes which are shown in Fig. 1. The lower catchment of the basin still exposed to flooding in the post-dam period due to high discharge released from the upstream dam during peak monsoon. Recently Lower Damodar area observed major and moderate floods in years i.e. 1990, 1991, 1993, 1994, 1995, 1996, 1998, 1999, 2000, 2006, 2007, 2009, 2011, 2013, 2015 and 2017. The reach of the Damodar river which is selected for the modeling purpose in the present study is highlighted with red line boundary as shown in Fig. 1. Durgapur barrage is the starting point of this area. It is the last hydraulic structure that controls the river flow in the lower reach of the Damodar river and also due to the availability of data like discharge and gauge; this site was chosen as starting point in hydrodynamic modeling. Daily gauge data measured at the Jamalpur, Harinkhola and Champadanga gauging stations were collected from Central Water Commission (CWC), Damodar Valley Corporation (DVC) and Irrigation and Waterways Department of West Bengal. High spatial resolution DEM and satellite imagery were procured from National Remote Sensing Centre Hyderabad for geometry data preparation in the model.

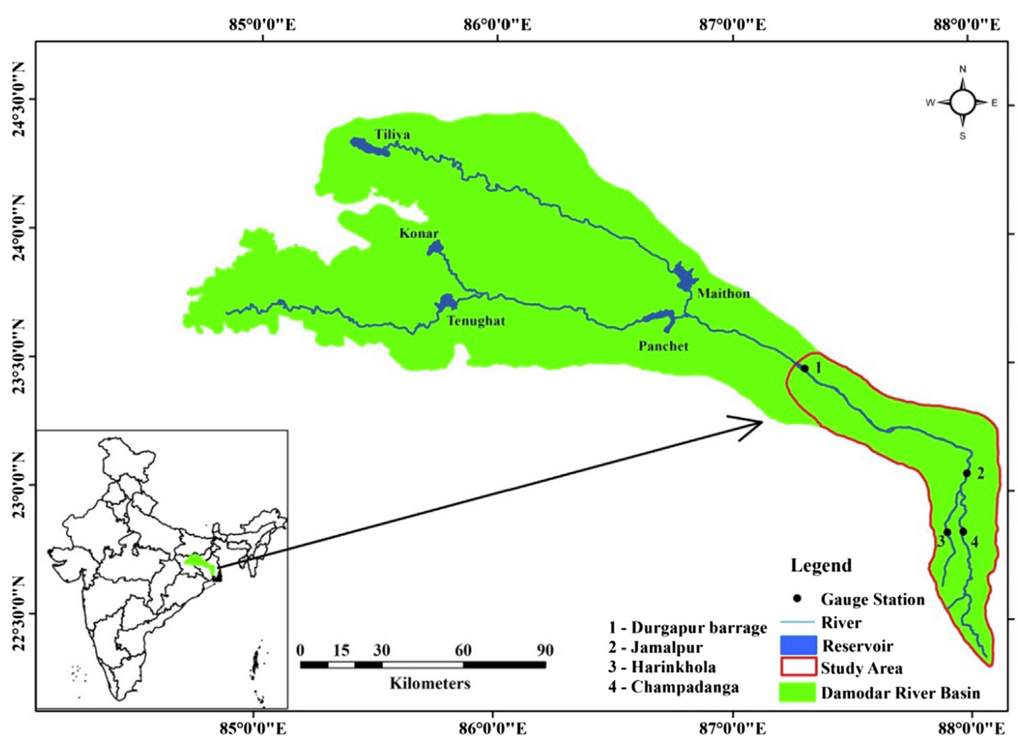

Fig. 1. Location map of Study area in Damodar river basin.

3. Research methodology

The purpose of this modeling study is to identify the flood vulnerability areas in the lower Damodar river basin. The research methodology of the present work is described in step by step manner in this section. The present study initiated with collection of information from previous literature, reports, field surveys and data from various sources government agencies. The data used in the study is already discussed in the previous section. After data collection preprocessing of data was performed. The next step was the preparation of various input geometry data (river network, bank line) for the hydrodynamic model in an Arc-GIS environment using high-resolution satellite imagery. The hydrodynamic model used DEM extracted cross-sections, which were 476 in total number for flood year. Out of which 158 cross-sections on the lower Damodar river from Durgapur barrage to bifurcation point of Damodar river, 183 numbers of cross-sections on Amta Damodar, 117 cross-sections on Mundeswari river and 18 cross-sections on the branch of Amta Damodar river. The spacing between the river cross sections were varied from 205 m to 1200 m with the aim of properly defining the variations in the physical shape and size of the river, along with the physical and mathematical needs of the hydrodynamic model. Knowledge regarding the rise of water level in the river during peak flow is very important which is the difference in peak water level during the flood to the water level in the dry season. Fieldwork was conducted during post-monsoon season in November 2018 to estimate the water level in a river in corresponding season. Fig. 2(a–c) shows the photographs of fieldwork done during November 2018 with survey area. The measured depths of water in the river were then deducted from the observed water surface elevation to get the corresponding rise in peak season for available gauge station. Hydrodynamic modeling was performed by running MIKE HYDRO RIVER for the 2007 and 2009 monsoon periods to simulate gauge and discharge data at different cross-sections of the selected reaches of Damodar river. Model was calibrated for the Manning's coefficient of roughness (n) and validated with ground data and field photographs. Further, the efficiency of the model estimated by the index of agreement "d" is presented in Eq. (1). Index of agreement (d) is used in the present work because it work more precisely for peak flows [31]. Based on the model output flooding hotspots were demarcated. The flowchart of overall research methodology is shown in Fig. 3

$$d = 1 - \frac{\sum_{i=1}^{i=N}(O_i - M_i)^2}{\sum_{i=1}^{i=N}\left(\left|M_i - \bar{O}\right| + \left|O_i - \bar{O}\right|\right)^2} \tag{1}$$

where O_i and M_i are observed field data and model simulated data respectively, $\bar{O}$ is the observed data mean, N is the total number of observations in the observed field data time series, and i is the number of data points.

4. Result and discussion

4.1. Hydrodynamic modeling

1-D hydrodynamic model (MIKE HYDRO RIVER) was used in the present study. Model fully solves the St. Venant Equations, which is a combination of conservation of mass and conservation of momentum equations [32]. Continuity equations with lateral inflow and without lateral inflow are presented in Eqs. (2) and (3) respectively. Momentum equations considering all the terms is shown in eq. (4) and momentum eq. without lateral inflow, wind shear, eddy losses and assuming momentum distribution coefficient β = 1 is shown in Eq. (5).

Continuity equation

$$\frac{\partial Q}{\partial x} + \frac{\partial A}{\partial t} = q \tag{2}$$

Fig. 2. (a) Measurement of water depth in dry Post-monsoon at Jamalpur; (b) Elevation measurement by GNSS at Binigram near river bank; (c) Height of river bank from wetted elevation in dry post-monsoon at Amta.

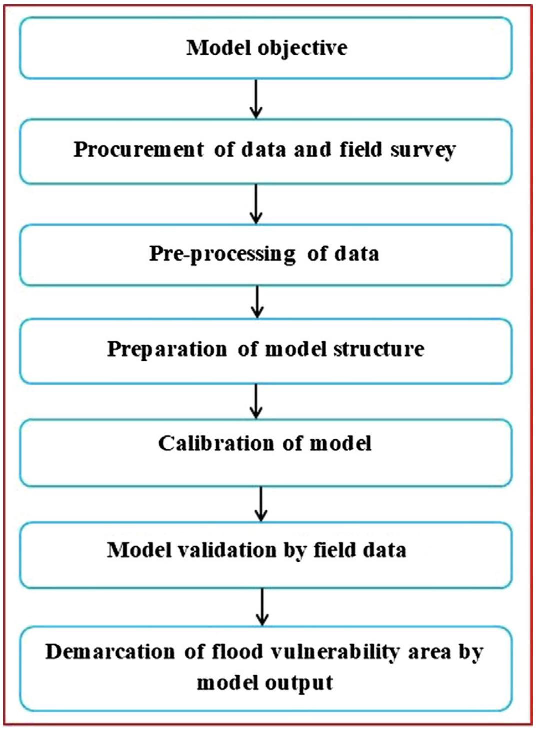

Fig. 3. Flowchart of the overall research methodology.

Neglecting lateral inflow

$$\frac{\partial Q}{\partial x} + \frac{\partial A}{\partial t} = 0 \tag{3}$$

Momentum equation

$$\frac{\partial Q}{\partial t} + \frac{\partial(\beta Q^2/A)}{\partial x} + gA\left(\frac{\partial y}{\partial x} - S_o + S_f + S_e\right) - \beta q v_x + W_f B = 0 \tag{4}$$

Ignoring lateral inflow, wind shear, eddy losses and assuming momentum distribution coefficient $\beta = 1$

$$\frac{1}{A}\frac{\partial Q}{\partial t} + \frac{1}{A}\frac{\partial(Q^2/A)}{\partial x} + g\left(\frac{\partial y}{\partial x}\right) - g\,(S_o - S_f) = 0 \tag{5}$$

where

Q = discharge (m^3/s), x = longitudinal distance along the channel (m), t = time (sec or h), A = cross-sectional flow area (m^2), y = water depth (m), g = acceleration due to gravity (m/s^2), q = lateral inflow per unit length (m^2/s), S_o = bottom slope, S_f = friction slope, S_e = eddy loss slope, β = momentum distribution coefficient, B = width of the channel at the water surface (m), W_f = wind shear factor (m^2/s^2), v_x = velocity of lateral flow in the direction of channel flow (m/s).

The St. Venant equations are partial differential equations which can be used in any practical problem with the help of the numerical method. Partial differential equations solved in numerical methods by performing the calculation on a grid placed over space–time (x-t) plane. Numerical schemes transform the governing partial differential equations into a set of algebraic finite- difference equations. A finite difference method may be employed either an explicit scheme or an implicit scheme for the solution. The difference between explicit and implicit method can be differentiated based on their stability, implicit conditionally stable for all the time steps on the other hand explicit method numerically stable only for time steps less than a critical value determined by the courant condition. With the help of Computer programming the implicit method can be solved even though it was mathematically more complicated [33,34].

MIKE HYDRO RIVER hydrodynamic model used six-point Abbott and Lonescu [35] implicit finite difference numerical schemes to solve the St.-Venant equations. The computational efficiency of numerical simulation is vastly reliant on the computational grid of the model applied during simulation. The computational grid of the model consists of alternate discharge point and water level point which is created automatically on the basis of the user necessities. Discharge point always placed halfway between adjacent water level point and at structures, while water level point located at cross-sections. In this modeling work the spacing between the river cross sections were varied from 205 m to 1200 m with the aim of properly defining the variations in the physical shape and size of the river, along with the physical and mathematical needs of the hydrodynamic model. The closeness of river cross-sections vary inversely with river curve, spacing was more for straight shape and less for curved shape.

Daily discharge data at Durgapur barrage was used as upstream boundary condition and Q/h was curve used as a boundary condition in downstream of the model. Additionally, 2007 and 2009 flood events return period were calculated by annual peak discharge from 1958 to 2017 at Durgapur barrage (Fig. 4). The return

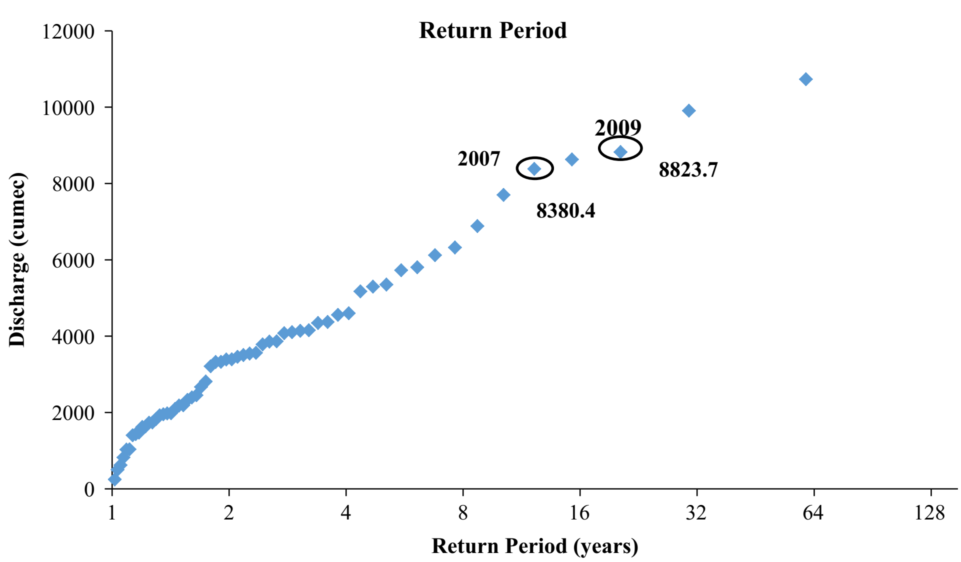

Fig. 4. The return period of the annual peak discharge.

period estimated for 2007 and 2009 flood events from time series of annual peak discharge was 20 years and 12 years respectively. The 2007 and 2009 flood events were chosen for this study against the year 1978 and 1959 because these events occurred quite recently in comparison to both and also river morphology, land use and land cover (LULC), etc. changed in due course of time. Taking care of numerical difficulties and other problems during low flow, an initial condition water depth of 0.5 m was provided in the model which was the minimum water depth set in the model. [32]. River network and starting and ending chainage of each stream in MIKE HYDRO RIVER model shown in Fig. 5(a) and (b) shows the location of the gauge station and extracted cross-section from DEM on the Google Earth image. All the data related to model set-up is presented in Table 1.

Table 1
Model Simulation Criteria.

Hydrodynamic model	1-D MIKE HYDRO RIVER
DEM resolution	CARTOSAT 1 = 10 m
Satellite imagery resolution	LISS IV = 5 m
Simulation period	1st July to 17th October 2007 and 1st July to 15th October 2009
Cross-section spacing	205–1270 m
Total cross-section	476
Time step	1 min
Output data Storage frequency	180 time step = 180 min
Upstream Boundary condition	Daily Discharge Data
Downstream Boundary condition	Q/H curve
Initial condition	0.5 m water depth
Manning's roughness coefficient (n)	0.02–0.045

4.2. Calibration

The 1-D hydrodynamic model was run for two high-magnitude flood event one from the period 1st July to 17th October 2007 and other from the period 1st July to 15th October 2009. Simulation of gauge and discharge data was performed at different cross-sections of the selected reach of Damodar river. Daily discharge data at Durgapur barrage used as input in upstream boundary condition and Q/h curve used as a boundary condition in downstream of the model [32]. Manning's coefficient of roughness (n) was used as a model calibration parameter. One minute as the computational time step and 207 m – 1270 m cross-sections spacing as a computational grid was set up for the model.

In the initial stage, approximations for the Manning's coefficient of roughness (n) for the channel were taken from available literature, i.e. [36] for a similar area. The Manning's roughness coefficient (n) value was varied from 0.02 to 0.045 during the model calibration process [36,37]. The efficiency of the model was measured using daily water depth data at the Jamalpur, Harinkhola and Champadang gauging stations. In the present study, authors have used high resolution DEM data for geometry to extract river cross-section. But, during DEM preparation, river bed level is not captured, instead water level of the river got captured. So in the present study, to avoid this level difference error, the authors have taken the environmental flow water level data through field survey (Fig. 2a–c) and this level is deducted from the observed data and remaining water depth is used for water rise in calibration process at the gauge site. Considering this, the model was simulated and the model output (water depth) was compared the observed water depth. For Manning's n value of 0.03, the model predicted data at selected gauging site was very close to observed field data. Figs. 6–8 shows a comparison between observed and

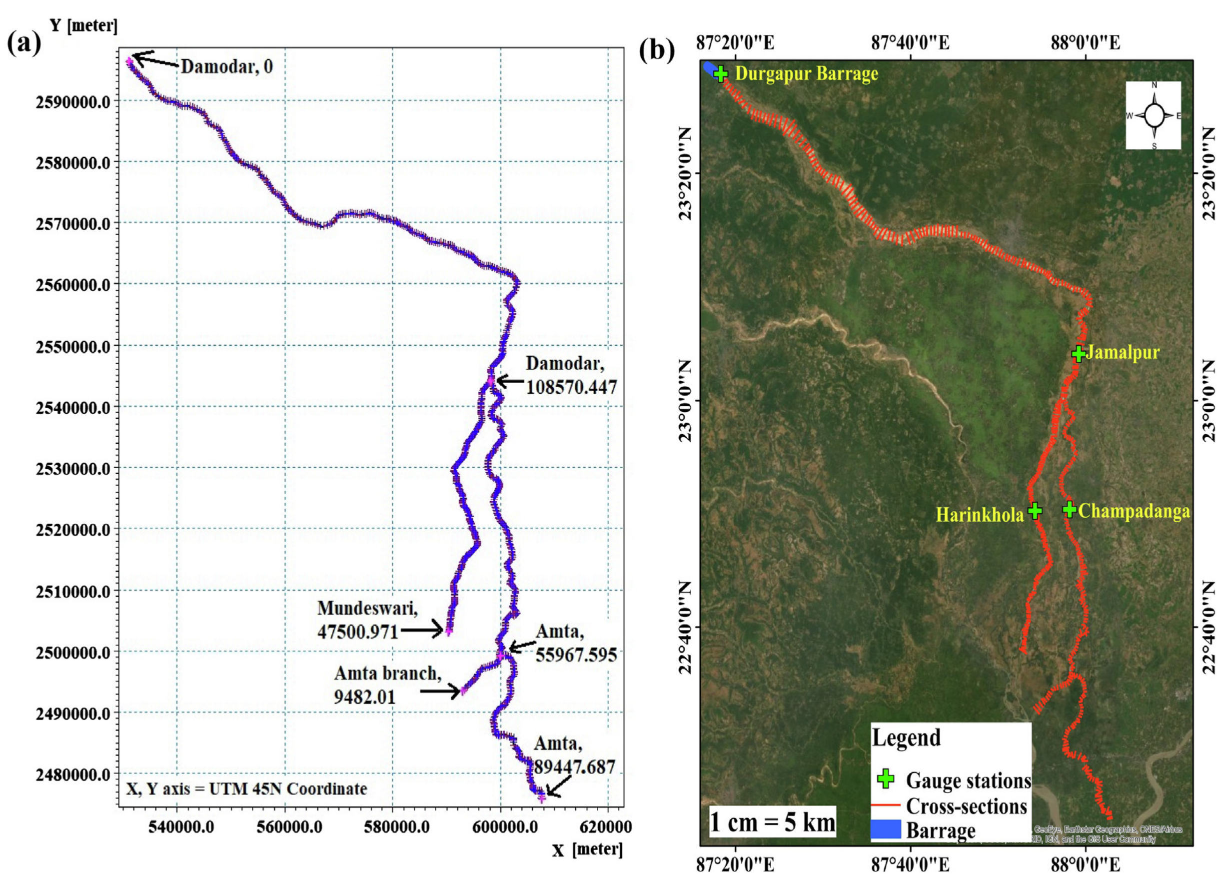

Fig. 5. (a) Location of river network and chainage in MIKE HYDRO RIVER (b) Location of gauge station, river and extracted cross-section on Google Earth image.

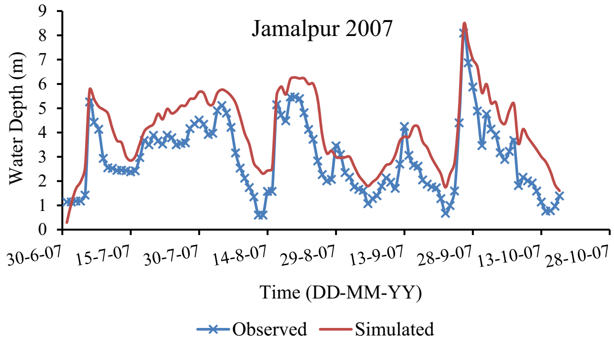

Fig. 6. Observed and Simulated water depth at Jamalpur site in 2007.

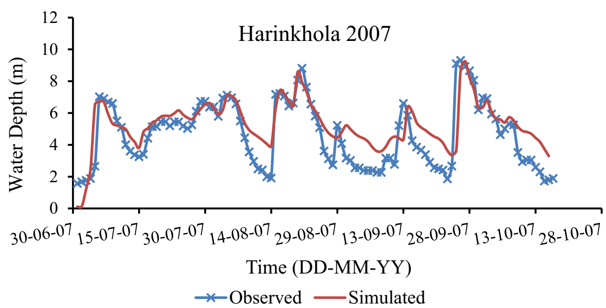

Fig. 7. Observed and Simulated water depth at Harinkhola site in 2007.

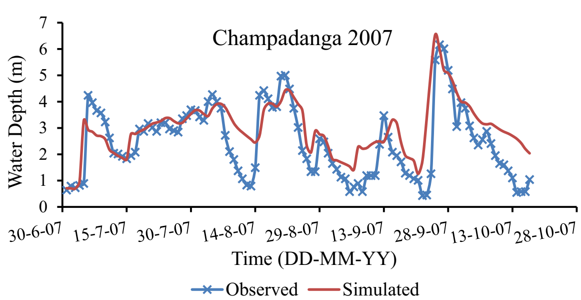

Fig. 8. Observed and Simulated water depth at Champadanga site in 2007.

model simulated water depth at Jamalpur, Harinkhola and Champadanga gauging sites for the year 2007 and Figs. 9–11 shows a comparison between observed field data and model simulated water depth data at Jamalpur, Harinkhola and Champadanga gauging sites for the year 2009. In the present study only main streams

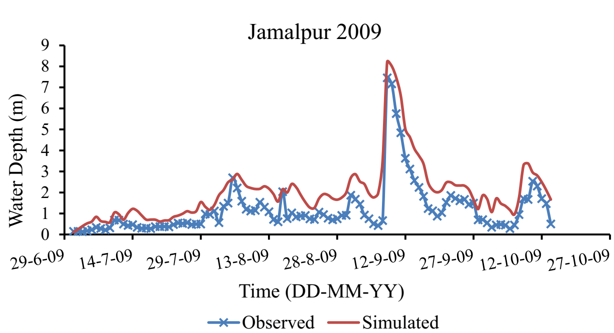

Fig. 9. Observed and Simulated water depth at Jamalpur site in 2009.

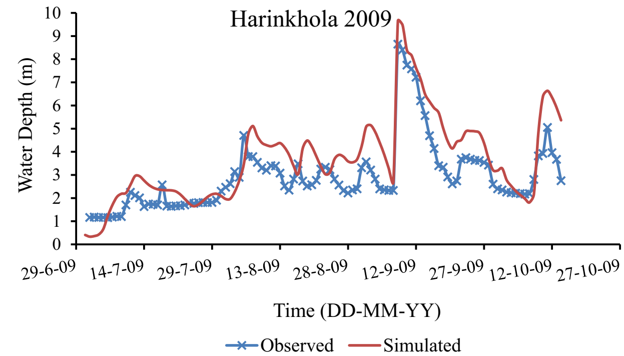

Fig. 10. Observed and Simulated water depth at Harinkhola site in 2009.

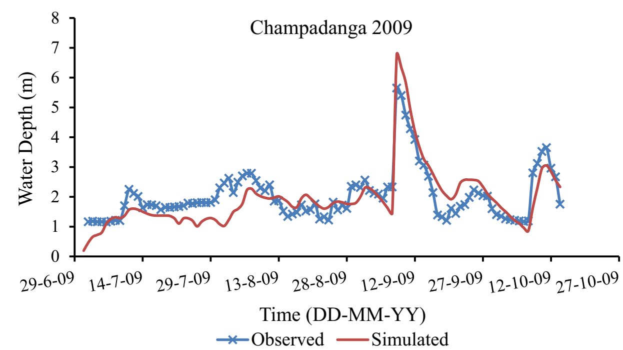

Fig. 11. Observed and Simulated water depth at Champadanga site in 2009.

are considered and after bifurcation of Damodar river in Mundeswari and Amta Damodar river, many small distributary are generated which is active only during peak flow time and have been not considered in the present study. One such narrow stream generated at the upstream of Mundeswari river before Harinkhola gauge site and the same stream meets at the downstream of Harinkhola gauge site in Mundeswari river that minor stream highlighted in Fig. 12. That's why, the water depth obtained from the model output is higher than the observed data in some segments when compared with the segments on the other side of the gauge. Also in the present study authors considered reach as a lumped model and this type of model generally over predict.

4.3. Validation

In flooding conditions, it was challenging to get the data for validation because most of the areas were submerged during that period and also flood events for the present study occurred in past times some years ago. For the present condition, field visit data and photographs at major locations were used for validation. Gauge stations were available for validation of hydrodynamic simulation data in lower Damodar river basin. Remaining was validated with the field visit photographs. Field visit photographs with the flood water levels marks on the banks and maximum rise in the past were considered for validation of simulation model results. Figs. 13 and 14 show the field validation of model predicted water depth at Jamalpur and Udaynarayanpur. The model output at three gauge locations with index of agreement and observed water depth data for years 2007 and 2009 were in close agreement and similar results were reported by [8] is listed in Table 2. The various hydraulic parameters of the lower Damodar river basin, including the water surface slope, flow velocity, flow width, flow area, hydraulic radius, conveyance and Froude number,

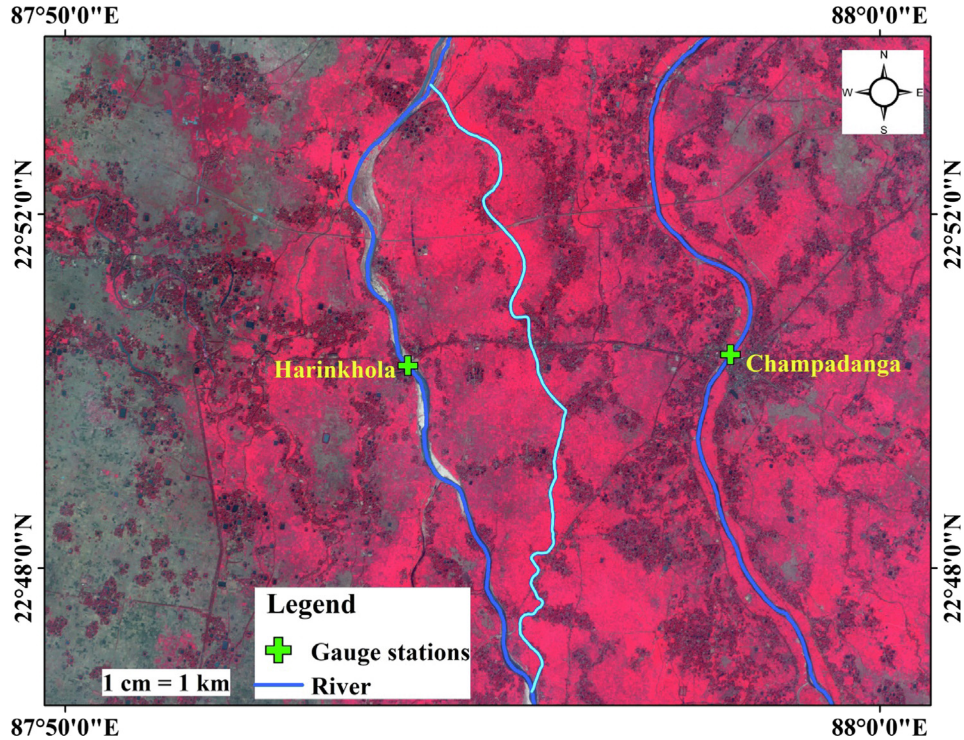

Fig. 12. Map showing minor stream of Mundeswari river upstream to Harinkhola gauge site.

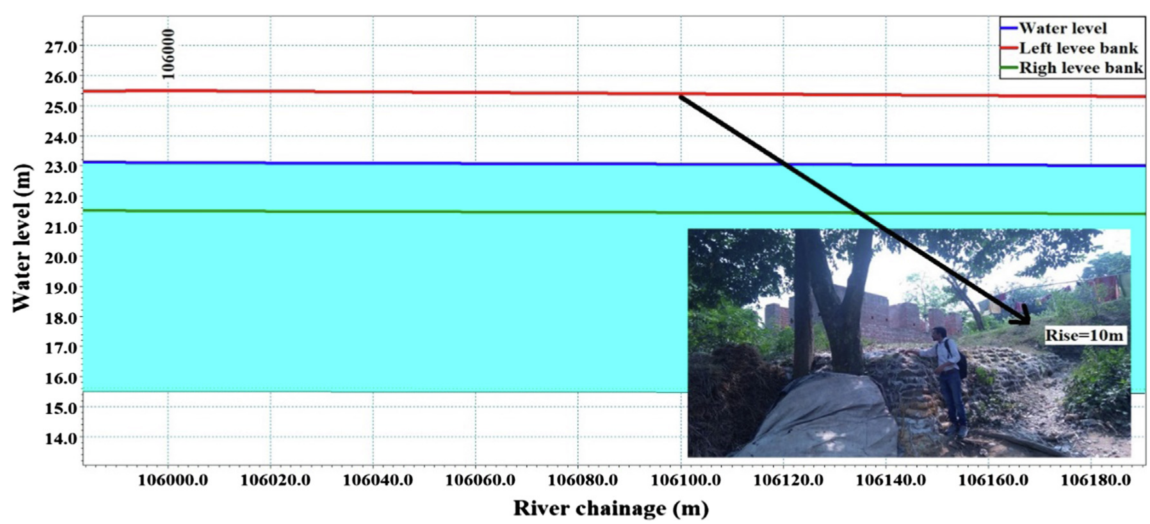

Fig. 13. Map showing field observation with model output at Jamalpur.

were generated through a 1D hydrodynamic model simulation along the river reach and these are supportive in designing flood protection measures and development of flood inundation map of the lower Damodar river basin. Water level profile for Damodar and Mundeswari river with left and right levee bank is shown in Fig. 15 whereas water level profile for Damodar and Amta river shown in Fig. 16. The simulated water surface profiles for the selected rivers using MIKE HYDRO RIVER model quite useful for identifying the weak levee points for flood prevention. From the water level profile, it was observed that spilling of water from river bank mostly occur in downstream section of Mundeswari and Amta reach because after bifurcation point, the river cross-section are gets narrower. Flow velocity obtain from the model output depict overtopping the river embankments due to the formation of turbulence in the runoff [38] and this velocity time series predicted by model for 2007 and 2009 at three gauge location are shown in Figs. 17 and 18. Flood level marks with flood-affected settlements locations at Champadanga gauge station during ground validation shown in Fig. 19(a–c). These predicted hydraulic parameters determine the competence of the model, which aid in evaluating the morphological conduct of the water flow during a flood. It is further observed that the model performs quite well in simulating the peak flows that is of supreme importance in flood modeling. The simulation results based on the hydrodynamic modeling can be improved by using a two-dimensional model, particularly in the plain areas of the lower.

Earlier study [8] used 90 m SRTM DEM (low resolution) data for developing 1-D hydrodynamic model whenever the river

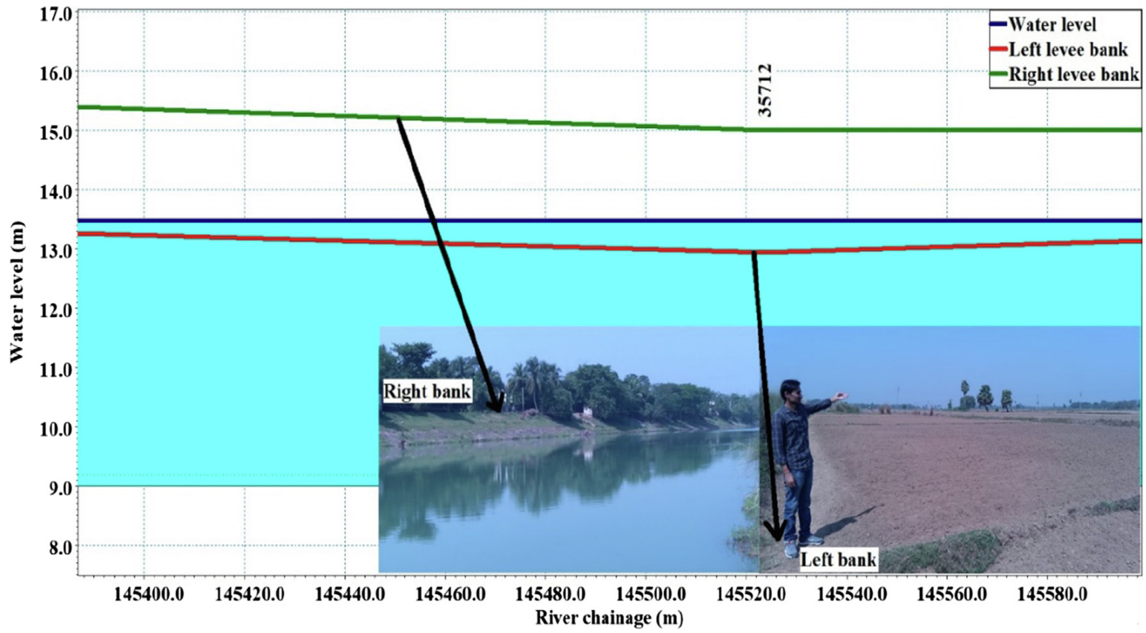

Fig. 14. Map showing field validation with model output at Udaynarayanpur.

Table 2
Model output at gauge location.

Parameters		Jamalpur 2007	Jamalpur 2009	Harinkhola 2007	Harinkhola 2009	Champadanga 2007	Champadanga 2009
Discharge (m^3/s)		7918.01	8163.82	5660.16	5808.06	2111.19	2168.34
Velocity (m/s)		3.314	3.35	2.608	1.56	3.19	3.355
Water depth (m)	**Observed**	8.09	7.45	8.92	8.64	6.16	6.35
	Simulated	8.42	8.22	9.26	9.56	6.55	6.77
Flow area (m^2)		2388.92	2432.66	2181.63	2211.28	708.6	712.58
Flow width (m)		464.15	466.65	371.66	388.044	353.49	354.94
Hydraulic radius (m)		6.93	6.97	8.439	8.46	2.99	2.989
Conveyance		286,069	296,023	301,316	306,129	48,968	49,287
Water level Slope		0.003	0.003	0.001	0.001	0.002	0.002
Froude Number		0.604	0.579	0.287	0.294	0.681	0.65
Index of agreement (d)		0.842	0.886	0.839	0.886	0.831	0.91

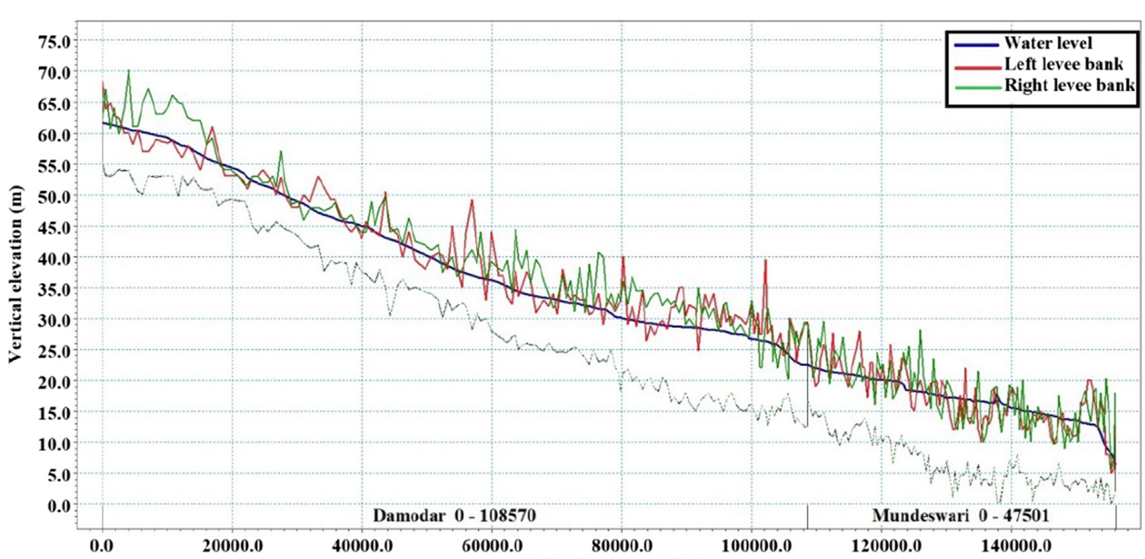

Fig. 15. Map showing water level profile for Damodar and Mundeswari river.

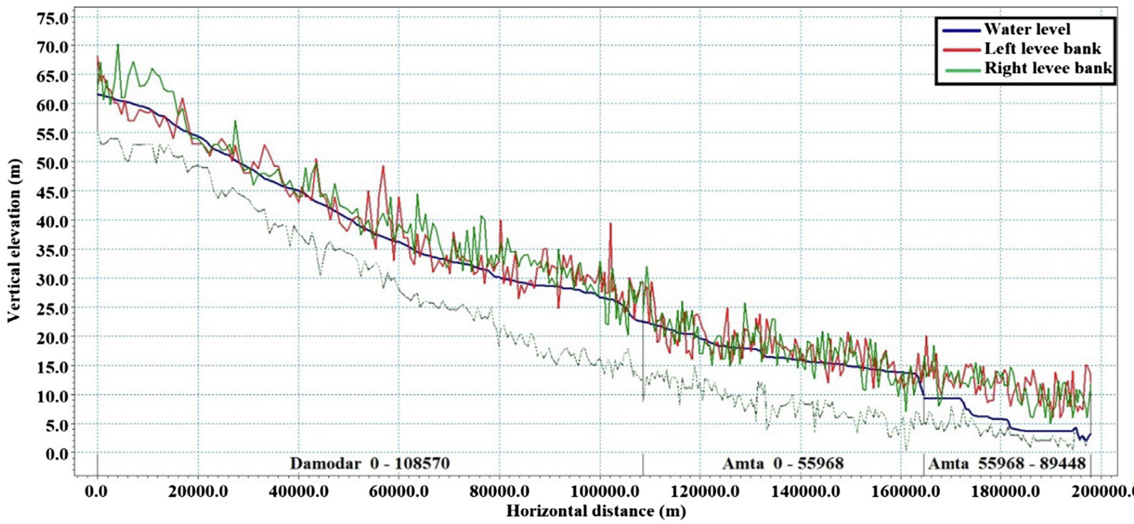

Fig. 16. Map showing water level profile for Damodar and Amta river.

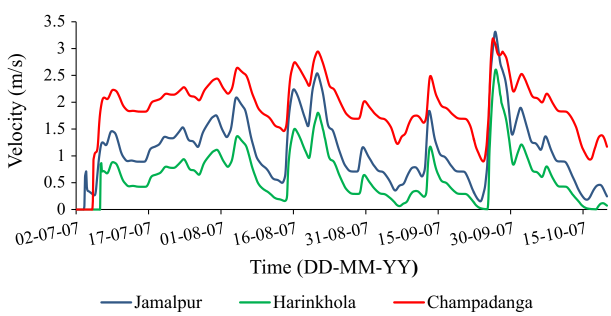

Fig. 17. Model predicted flow velocity time series at three gauge location for 2007.

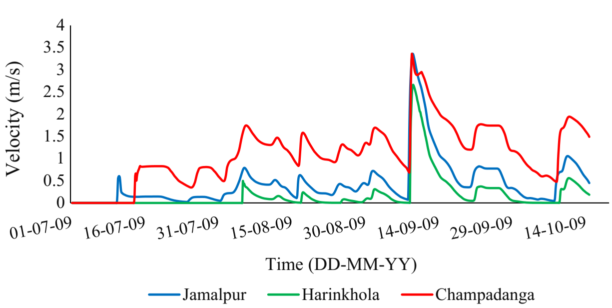

Fig. 18. Model predicted flow velocity time series at three gauge location for 2009.

cross-section is very narrow, there lower resolution data will not able to provide the precise river cross-section at that locations and it affect the model output whereas the present approach (high resolution of 10 m Cartosat-1 DEM data) can identify the more precise cross-section compared to earlier. [8,39] used contour map of 20 m interval for DEM preparation which was used as geometric data in the hydrodynamic model due to unavailability of survey, higher-resolution data. This lack of accurate data effected the model output and hence the results obtained is not satisfactory. They reported that large-scale uncertainties will definitely be introduced into the DEMs produced from such sparse data. Whereas in the present study, all the above issues have been taken care of. In the present study, authors used high-resolution DEM (10 m Cartosat-1 DEM), high-resolution remote sensing satellite imagery data, reconnaissance survey was done before developing the model to validate the river cross-section obtained from the satellite image. The authors have also carried out ground truth verification (validation) of the model output. The present study used latest version of MIKE 11 which is MIKE HYDRO RIVER for Hydrodynamic model development. Calibration, ground validation of the simulated results, latest updated model, high-resolution remote sensing satellite imagery data was used during model development for making the model more robust. The results are better than the earlier studies. Based on the Hydrodynamic Model maximum water depth map was prepared for the lower Damodar and using this map flooding hotspot nearby river were demarcated having area 859,908 m^2, 22,106,210 m^2, 6,550,166 m^2 near the Damodar, Mundeswari and Amta Damodar rivers respectively as shown in Fig. 20(a and b). Authors acknowledge that model performance influenced by the composite interaction among the selected parameters like locations, model inputs and the physical features of the model area. So the flooding hotspot which was identified based on the 1-D hydrodynamic model represents only those areas which likely under the model domain. From the model output and also with field validation, it is observed that areas downstream to the bifurcation point of the Damodar river are more vulnerable to flooding. During the flood period, flood water spill over both banks of Mundeswari and Amta Damodar and subsequently area nearby the river get inundated. Topography shows the flood affected areas are at very low levels compared to the river bank, so once the water overtopped the bank of the river, it easily spreads in the larger portion of area. Encroachment in the riverine system for agricultural purposes, changes in LULC due to the recent developments and activation of local minor distributaries during peak monsoon season with inadequate capacity in these low laying areas aids the spatial extent of flooding.

5. Conclusions

The present study utilized a one-dimensional hydrodynamic modeling approach to identify the flood vulnerability sites for high discharge release by Durgapur barrage during peak monsoon of 2007 and 2009 years. Taking into consideration proper variations in the physical shape of the river, along with the physical and mathematical needs of the hydrodynamic model 476 DEM extracted cross-sections were used in MIKE HYDRO RIVER model. For Manning's n value of 0.03, the model predicted data at selected gauging site was very close to observed field data and also the index of agreement (d) shows good agreements between model

Fig. 19. (a) Water depth measurement during post-monsoon season at Champadang gauge station (b) Map showing flood level marks at Champadang gauge station (c) Map showing flood-affected settlement very close to the riverbank.

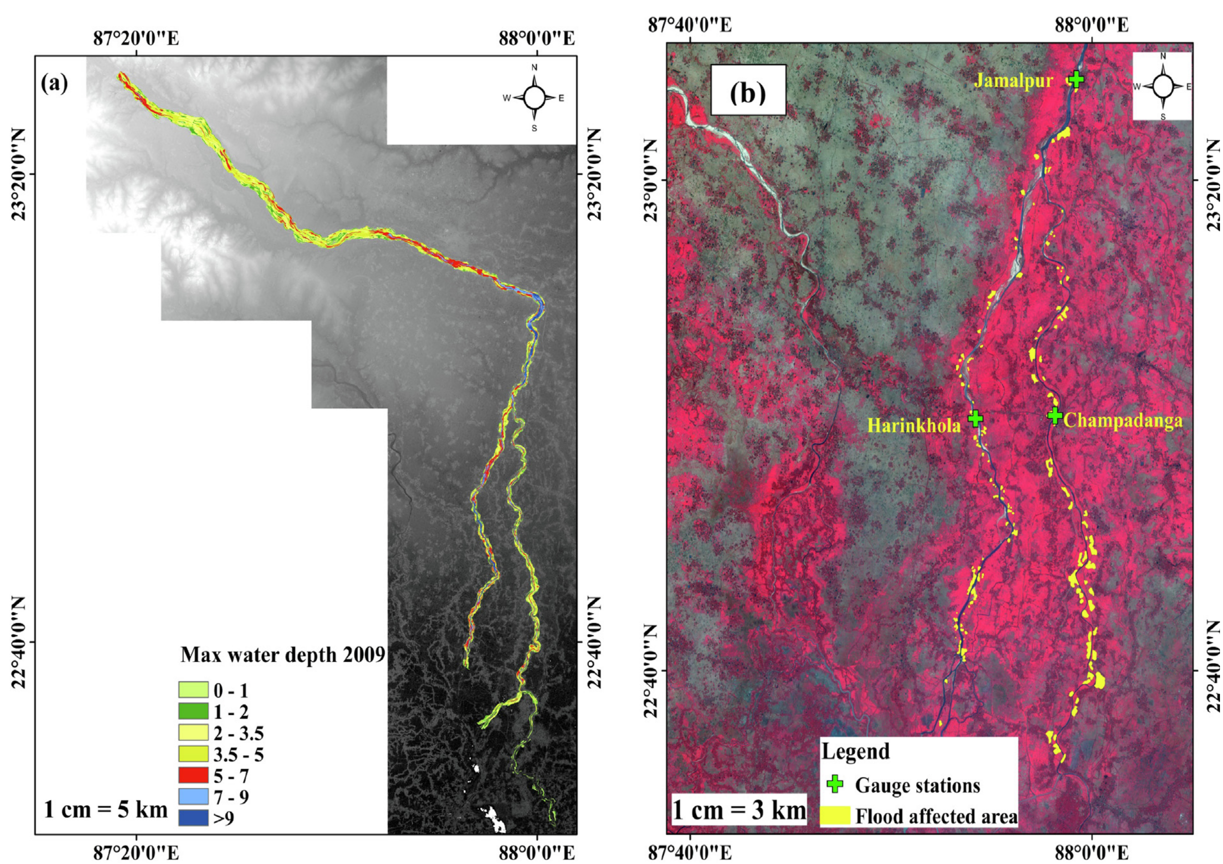

Fig. 20. (a) Maximum water depth map by 1-D model overlaid on high-resolution DEM (b) Flooding hotspot overlaid on high-resolution satellite imagery.

output and observed data at the Jamalpur, Harinkhola and Champadanga gauging stations. Based on predicted water surface profile by the hydrodynamic model, it was observed that areas downstream to the bifurcation point of the Damodar river are more vulnerable to flooding. The flooding risk hotspots identification in lower Damodar river of eastern India due to riverine flooding of the Damodar river was successfully achieved in present study by performing 1-D modeling. Findings of the study shows that much of the flood affected areas are at very low levels compared to the river bank, so once the water overtopped the bank of the river, it easily spread in the larger part of area and presence of large plain areas with small variations in elevation creating problems of draining out water from different parts of the floodplain. So taking into consideration these issues a detailed study in the form of 2-D modeling of the area between Mundeswari and Amta Damodar river as an extension to the present study is the need of the hour. The authors will incorporate all these issues in the proposed 2-D model as the extension of the present study by linking the 1-D model output for defining boundary condition of 2D model. Authors believe that the present study can immensely aid the engineers and planners in policy decisions for combating the floods in the lower Damodar basin for sustainable development.

Acknowledgments

The fieldwork carried out and high-resolution DEM data procurement were funded by FRS project (FRS (120)/2017-18/ME) of Dr. V.V. Govind Kumar, IIT(ISM), Dhanbad. Authors sincerely acknowledge Damodar Valley Corporation Maithon, Central Water Commission (CWC), Irrigation and Waterways Directorate, Government of West Bengal for providing the essential data for the study and technical support received from faculty of IIT(ISM) Dhanbad and DHI India regarding MIKE HYDRO RIVER hydrodynamic model.

References

[1] Jain SK, Singh RD, Jain MK, Lohani AK. Delineation of flood-prone areas using remote sensing techniques. Water Resour Manage 2005;19(4):333–47. https://doi.org/10.1007/s11269-005-3281-5.
[2] Kale VS. The spatio-temporal aspects of monsoon floods in India: implications for flood hazard management. Disaster management. University Press, Hyderabad; 2003. p. 22–47.
[3] Mohapatra PK, Singh RD. Flood Management in India. In: Flood problem and management in South Asia. Netherlands: Springer; 2003. https://doi.org/10.1007/s12665-016-5297-y.
[4] Alavi SR, Lay EN, Makhmali ZA. A CFD study of industrial double-cyclone in HDPE drying process. Emerg Sci J 2018;2(1):31–8. https://doi.org/10.28991/esj-2018-01125.
[5] Pramanik N, Panda RK, Sen D. One dimensional hydrodynamic modeling of river flow using DEM extracted river cross-sections. Water Resour Manage 2010;24(5):835–52. https://doi.org/10.1007/s11269-009-9474-6.
[6] Torbizadeh A, Tahershamsi A, Tabatabai MRM. Field study of morphological parameters in step-pool streams. Civ Eng J 2018;4(8):1930–8. https://doi.org/10.28991/cej-03091127.
[7] Ghosh S, Guchhait SK. Dam-induced changes in flood hydrology and flood frequency of tropical river: a study in Damodar River of West Bengal, India. Arabian J Geosci 2016;9(2):1–26. https://doi.org/10.1007/s12517-015-2046-6.
[8] Timbadiya PV, Patel PL, Porey PD. One-dimensional hydrodynamic modeling of flooding and stage hydrographs in the lower Tapi River in India. Curr Sci 2014;106(5):708–16. , http://www.jstor.org/stable/24099969.
[9] Movahedi A, Kavianpour MR, Yamini OA. Evaluation and modeling scouring and sedimentation around downstream of large dams. Environ Earth Sci 2018;77(8):320. https://doi.org/10.1007/s12665-018-7487-2.
[10] Aminoroayaie Yamini O, Kavianpour MR, Mousavi SH, Movahedi A, Bavandpour M. Experimental investigation of pressure fluctuation on the bed of compound flip buckets. ISH J Hydraulic Eng 2018;24(1):45–52. https://doi.org/10.1080/09715010.2017.1344572.
[11] Machekposhti KH, Sedghi H, Telvari A, Babazadeh H. Flood analysis in Karkheh River basin using stochastic model. Civil Eng J 2017;3(9):794–808. https://doi.org/10.21859/cej-030915.
[12] Jung Y, Merwade V. Uncertainty quantification in flood inundation mapping using generalized likelihood uncertainty estimate and sensitivity analysis. J Hydrol Eng 2011;17(4):507–20. https://doi.org/10.1061/(ASCE)HE.1943-5584.0000476.
[13] Pappenberger F, Matgen P, Beven KJ, Henry JB, Pfister L. Influence of uncertain boundary conditions and model structure on flood inundation predictions. Adv Water Resour 2006;29(10):1430–49. https://doi.org/10.1016/j.advwatres.2005.11.012.
[14] Quiroga VM, Kurea S, Udoa K, Manoa A. Application of 2D numerical simulation for the analysis of the February 2014 Bolivian Amazonia flood: application of the new HEC-RAS version 5. Ribagua 2016;3(1):25–33. https://doi.org/10.1016/j.riba.2015.12.001.
[15] Cook A, Merwade V. Effect of topographic data, geometric configuration and modeling approach on flood inundation mapping. J Hydrol 2009;377(1–2):131–42. https://doi.org/10.1016/j.jhydrol.2009.08.015.
[16] Hunter NM, Bates PD, Matthew S, Horritt MS, Wilson MD, et al. Simple spatially-distributed models for predicting flood inundation: a review. Geomorphology 2007;90:208–25. https://doi.org/10.1016/j.geomorph.2006.10.021.
[17] Werner MGF. A comparison of flood extent modeling approaches through constraining uncertainties on gauge data. Hydrol Earth Syst Sci 2004;8(6):1141–52. https://doi.org/10.5194/hess-8-1141-2004.
[18] Correia FN, Rego FC, Saraiva MDG, Ramos I. Coupling GIS with hydrologic and hydraulic flood modeling. Water Resour Manage 1998;12(3):229–49. https://doi.org/10.1023/A:1008068426567.
[19] Renyi L, Nan L. Flood area and damage estimation in Zhejiang, China. J Environ Manage 2002;66(1):1–8. https://doi.org/10.1006/jema.2002.0544.
[20] Bates PD, Wilson MD, Horritt MS, Mason DC, Holden N, Currie A. Reach scale floodplain inundation dynamics observed using airborne synthetic aperture radar imagery: data analysis and modelling. J Hydrol 2006;328(1–2):306–18. https://doi.org/10.1016/j.jhydrol.2005.12.028.
[21] Chatterjee C, Förster S, Bronstert A. Comparison of hydrodynamic models of different complexities to model floods with emergency storage areas. Hydrol Process 2008;22(24):4695–709. https://doi.org/10.1002/hyp.7079.
[22] Aronica G, Hankin B, Beven K. Uncertainty and equifinality in calibrating distributed roughness coefficients in a flood propagation model with limited data. Adv Water Resour 1998;22(4):349–65. https://doi.org/10.1016/S0309-1708(98)00017-7.
[23] Bates PD, De Roo APJ. A simple raster-based model for flood inundation simulation. J Hydrol 2000;236(1–2):54–77. https://doi.org/10.1016/S0022-1694(00)00278-X.
[24] Hsu MH, Fu JC, Liu WC. "Flood routing with real-time stage correction method for flash flood forecasting in the Tanshui River, Taiwan. J Hydrol 2003;283(1–4):267–80. https://doi.org/10.1016/S0022-1694(03)00274-9.
[25] Pappenberger F, Beven K, Horritt M, Blazkova S. "Uncertainty in the calibration of effective roughness parameters in HEC-RAS using inundation and downstream level observations. J Hydrol 2005;302(1–4):46–69. https://doi.org/10.1016/j.jhydrol.2004.06.036.
[26] Bates PD, Marks KJ, Horritt MS. Optimal use of high-resolution topographic data in flood inundation models. Hydrol Process 2003;17(3):537–57. https://doi.org/10.1002/hyp.1113.
[27] Dutta D, Herath S, Musiake K. Flood inundation simulation in a river basin using a physically based distributed hydrologic model. Hydrol Process 2000;14(3):497–519. https://doi.org/10.1002/(SICI)1099-1085(20000228)14:3<497::AID-HYP951>3.0.CO;2-U.
[28] Bhattacharyya K. The Lower Damodar River, India: understanding the human role in changing fluvial environment. Springer Science & Business Media; 2011.
[29] Ghosh S, Guchhait SK. Hydrogeomorphic variability due to dam constructions and emerging problems: a case study of Damodar River, West Bengal, India. Environ Dev Sustain 2014;16(3):769–96. https://doi.org/10.1007/s10668-013-9494-5.
[30] Ghosh S, Mistri B. Geographic concerns on flood climate and flood hydrology in monsoon-dominated Damodar River Basin, eastern India. Geography J 2015;2015. https://doi.org/10.1155/2015/486740.
[31] Legates DR, McCabe Jr GJ. Evaluating the use of "goodness-of-fit" measures in hydrologic and hydroclimatic model validation. Water Resour Res 1999;35(1):233–41. https://doi.org/10.1029/1998WR900018.
[32] MIKE. DHI 2017 1D Reference Manual.
[33] Te Chow Ven. Applied hydrology. New Delhi: McGraw-Hill; 1988.
[34] Dyhouse G, Hatchett J, Benn J. Floodplain modeling using HEC-RAS. USA: Bentley Institute Press; 2007.
[35] Abbott MB, Ionescu F. On the numerical computation of nearly horizontal flows. J Hydraul Res 1967;5(2):97–117. https://doi.org/10.1080/00221686709500195.
[36] Chow VT. Open-channel hydraulics. New York: McGraw-Hill; 1959.
[37] Kumar S, Kaushal DR, Gosain AK. Evaluation of evolutionary algorithms for the optimization of storm water drainage network for an urbanized area. Acta Geophys 2019;67(1):149–65. https://doi.org/10.1007/s11600-018-00240-8.
[38] Kumar S, Kaushal DR, Gosain AK. Hydrodynamic simulation of urban stormwater drain (Delhi city, India) using iRIC Model. J Appl Res Technol 2018;16(1):67–78. https://doi.org/10.22201/icat.16656423.0.16.1.704.
[39] Patro S, Chatterjee C, Singh R, Raghuwanshi NS. Hydrodynamic modelling of a large flood-prone river system in India with limited data. Hydrol Processes: Int J 2009;23(19):2774–91. https://doi.org/10.1002/hyp.7375.

Ravindra Kumar Singh, Research Scholar of Civil Engg. Dept. IIT (ISM) Dhanbad. I have done my B.Tech in Civil Engg. from BIT Sindri Jharkhand, India in 2012 and M. tech in Civil Engg. (Hydraulic Engg.) from IIT Roorkee, India. I have joined IIT (ISM) Dhanbad as Research Scholar in 2016. **1 First Author.**

Dr. Srinivas Pasupuleti Assistant Professor, Department of Civil Engineering, Indian Institute of Technology (ISM), Dhanbad, Dhanbad – 826004, Jharkhand. Life Member of Indian Society for Technical Education (MISTE), Indian Association of Hydrologists (MIAH), Indian Water Resources Society (MIWRS), Association of Hydrologists of India (MAHI), Indian Society for Hydraulics (MISH). Guidance at doctoral level -- 06 (In progress). **3 Corresponding Author.**

Dr. Vasanta Govind Kumar Villuri, Assistant Professor Geomatic Section, Department of Mining Engineering, Indian Institute of Technology(ISM), Dhanbad-826004, India. Life Time member of Indian Society of Geomatics (ISG), Indian Society of Remote sensing(ISRS), Dehradun and Mining Engineers Association of India (MEAI). Guidance at doctoral level -- 06 (In progress). Guidance at masters level ---15 (Completed). Guidance at undergraduate level--20 (Completed) **2 Co- Author.**

Rajesh Nune Scientist at ICRISAT Hyderabad, Telangana, India. Specialisation in the area of hydrology and water resources with over 9 years of experience in hydrology and water resources related disciplines. My expertise includes field monitoring, physically-based and conceptual modelling, assessing surface and groundwater water resources, relating catchment changes to stream flow, assessing current and future climate and anthropogenic impacts on hydrological systems, GIS and remote sensing. **4 Co- Author.**